Open Journal of Civil Engineering, 2022, 12, 247-269
https://www.scirp.org/journal/ojce
ISSN Online: 2164-3172
ISSN Print: 2164-3164

Microstructure of Fine Clay Soils Stabilized with Sugarcane Molasses

Narcisse Malanda[1], Nice Ngouallat Mfoutou[1], Erman Eloge Nzaba Madila[2], Paul Louzolo-Kimbembe[1,3*]

[1]National Upper Polytechnic School, Marien Ngouabi University, Brazzaville, Republic of Congo
[2]Department of Chemistry, Biochemistry and Physics and Hydrogen Research Institute, University of Quebec in Trois-Rivières, Trois-Rivières, Canada
[3]National Upper Education School, Marien Ngouabi University, Brazzaville, Republic of Congo
Email: *nar6malanda@gmail.com

How to cite this paper: Malanda, N., Ngouallat Mfoutou, N., Nzaba Madila, E.E. and Louzolo-Kimbembe, P. (2022) Microstructure of Fine Clay Soils Stabilized with Sugarcane Molasses. *Open Journal of Civil Engineering*, **12**, 247-269.
https://doi.org/10.4236/ojce.2022.122015

Received: March 21, 2022
Accepted: June 27, 2022
Published: June 30, 2022

Abstract

Sugar cane molasses has proved cohesive and excellent performance on soil aggregates (fine particles). However, the microstructure of consolidated soil by the molasses is not yet subjected to research. The analysis results of sample without molasses (0%) and consolidated samples at 8%, 12%, and 16% show that the molasses acts on the structure of clayey fine soil developing its microstructure of airy matrix type (sample without molasses (0%) to a microstructure of a qualified type, more solid. Consolidated samples to 8%, 12%, 16% of molasses). We also observe the presence of inter-aggregate pores (mesopores) of similar size in all samples. The results of porosimetrical analyses (BJH) of the sample without molasses and consolidated samples to 8%, 12%, and 16% show that simultaneous porous volumes of samples are reduced with the increasing of molasses quantity. This latter, therefore, acts on the porous volume (micropore < 2 nm and mesopore < 9 nm) by reducing them which really means, molasses occupies the porous volume of the sample. However, this sample seems not to have any effect on the size of mesopores 9 nm. Thus, this product induces the evolution of the soil structure towards the highly dense and condensed structure. Consequently, materials in consolidated soil by molasses will have mechanical properties far superior to those of materials consolidated soil without molasses.

Keywords

Microstructure, Consolidated, Clayey Fine Soil, Molasses of Sugar Cane, Mesopore, Micropore, Specific Surface Area

1. Introduction

The molasses considered as sugar cane remainder has proved a cohesive excellent performance on experiences on the consolidation of clayey soils in the town of Nkayi, in Republic of Congo (**Figure 1**). In fact, Malanda *et al*. (2017) have observed an increase in mechanic resistances of briquettes in condensed raw soil, consolidated by these molasses. It is evident that molasses bring a seed of cohesion to the soil as material [1] [2]. Now, the town of Nkayi has a clayey fine soil of level A1 [1] [2].

The behavior of this type of soil depends on the mineralogical nature of clayey materials and moisturizing fluid, knowing that molasses is really a viscous liquid separable in water and in process of the consolidation of fine soils and condensed soils. Thus, certain quantity of molasses is added to the content in the optimum Proctor water. However, the consolidation of fine soils by molasses finds certainly its explanation at the microstructural ladder of clayey soils of the town of Nkayi and chemical composition of molasses.

Sugar cane molasses being an organic solution, the capacity of soil consolidation by sugar cane molasses could be explained by the fixation of major organic constituents on clay of the soil. That fixation of constituents could go with the modification of soil microstructure and of the porosity, consolidating aggregates as a result of making out binders.

However, the microstructure of consolidated soil sugar cane molasses has not yet been subjected to research.

The aim of this study is to analyze the effects of soil consolidation by sugar cane molasses on the structure of clayey fine soil, examining the evolution of structure of consolidated soil according to the quantity of sugar cane molasses in the soil.

Figure 1. Sugar cane molasses poured out on roads with ground in the town of Nkayi (Picture taken on the ground) [Field photo].

Electronic microscopy of scanning is employed to examine the texture, structure, and quality of pores [3] [4]. The method BJH of nitrogen adsorption is employed to quantify the porosity [5] [6] [7].

2. Materials and Methods

2.1. Study Area

The town of Nkayi where the studies were carried out is located about 250 km from Brazzaville, the capital city of the Congo. The study area extends from 4˚9'56"S longitude and 13˚17'34"E latitude (**Figure 2**).

2.2. Materials

Sugar cane molasses and fine clayey soil from the town of Nkayi, Republic of Congo are the basic materials of our study.

2.2.1. Soil Sample

The results of some geotechnical tests performed on the soil are presented in **Table 1**. According to the triangular Taylor chart of the soil sample (**Figure 3**) and the particle size distribution, our soil is a fine clayey soil.

2.2.2. Sugar Cane Molasses

The sugarcane molasses in our study comes from the Société Agricole de Raffinage Industriel of sugar (SARIS-Congo), a sugar industry based in the city of Nkayi, Republic of Congo. The infrared chemical analysis of sugarcane molasses is shown in **Figure 4**.

Figure 2. Plan view of the city of Nkayi.

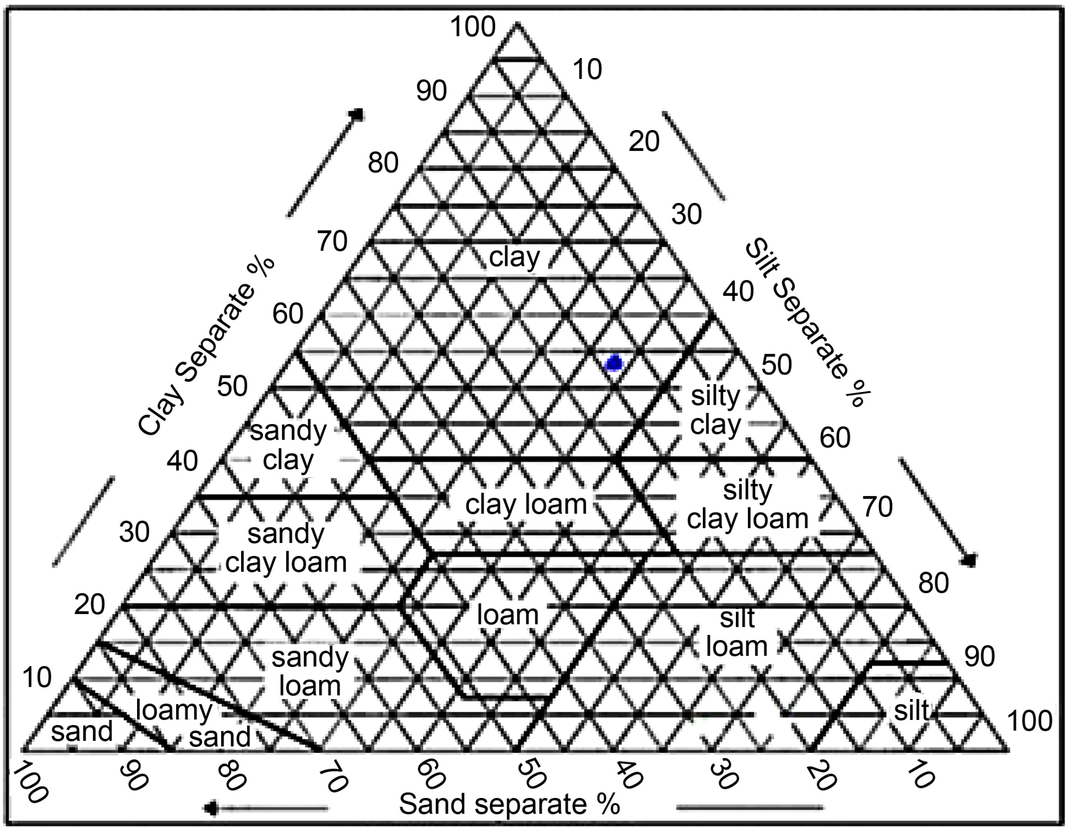

Figure 3. Taylor's triangular soil abacus.

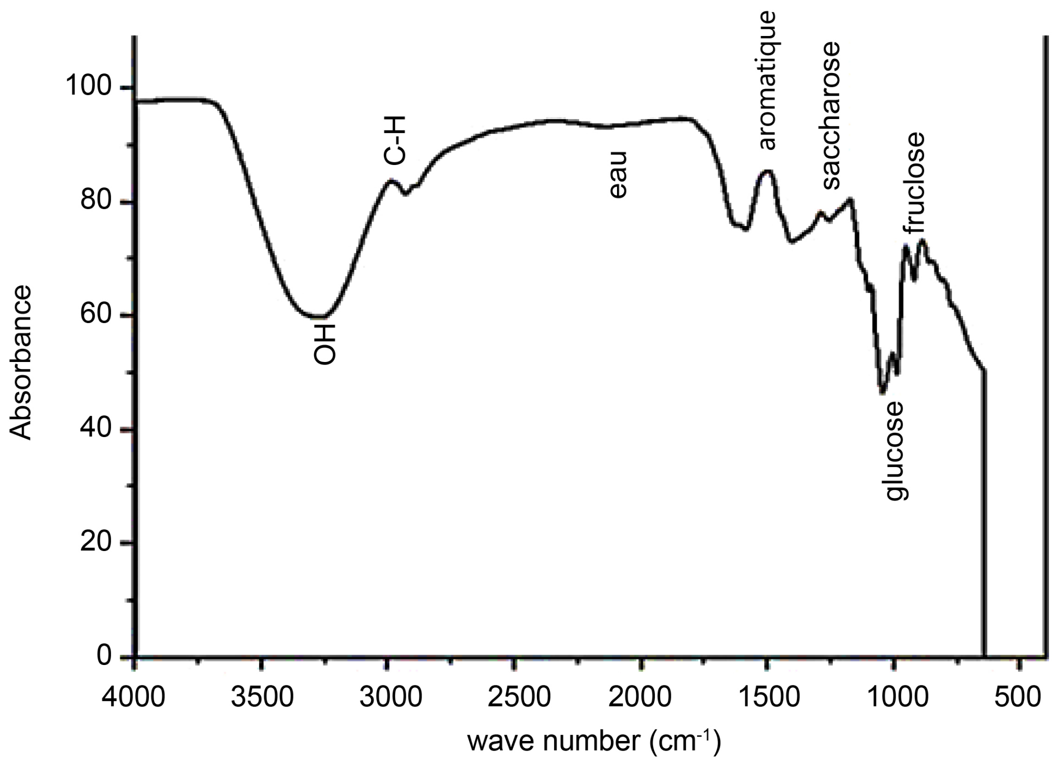

Figure 4. Infrared spectrum of sugar cane molasses.

Table 1. Geotechnical characteristics of the soil [1] [2].

Materials	particle size distribution				Limits of Atterberg			Compatibility		Methyleneblue
	% fines (<80 µm)	Clay < 2 µm	Silt between 2 µm et 63 µm	Sand between 63 µm et 2 mm	W_L (%)	W_p (%)	I_p (%)	γd (g/cm^3)	W (%) (OPM)	VBS (g/100g)
Soil taken at 1 meter depth	88	54	34	12	42	21	21	1.68	15	0.34

The region between 1200 and 1000 cm^{-1} is characteristic of glycosidic bonds (C-O-C) in combination with other modes such as: (C-O-H), (C-C), (C-H) of polysaccharides thus of sucrose. The region between 950 and 1200 cm^{-1} is characteristic of glucoses. The region between 950 and 400 cm^{-1} is characteristic of fructose. The peak at 1582 cm^{-1} is characteristic of the vibration of C=C bond of aromatic compound responsible for the coloring of sugar cane molasses like maltol and furaneol. Our sugarcane molasses is composed of sucrose, glucose, fructose, water and coloring compound such as maltol and furaneol, Phuong T. (2013), Belghiti (1993), Mathlouthi M. (1998) and Janekarn *et al.* (2020) made the same finding [8] [9] [10] [11].

2.2.3. The Making of the Consolidated Soil by Sugar Cane Molasses

Soil samples taken from the depth of the one meter, are grinded and revised at in a granular (granulometric) inferior to 400 micrometers (0.4 mm) after swing (**Figure 5(a)**). A mixture of dry soil and water at the height of 1.5 times, the limit of the soil liquidity is prepared, at the saturated pastry (content in initial water: wi = 1.5 w_L). Sugar cane molasses is added according to the wished quantity, everything is mixed with electrical stirring rod for 15 minutes. The homogenous pastry from this operation is put into test tube of dimension 1 × 1 × 1 cm^3 and dried in open air for a week. The obtained clay cakes (**Figure 5(b)**) are intended for different tests:

- A consolidated sample at 0% of molasses, that means without molasses (witness sample).
- A consolidated sample at 8% of sugar cane molasses.
- A consolidated sample at 12% of sugar cane molasses.
- A consolidated sample at 16% of sugar cane molasses.

Table 2 gives an example of water sharing out, molasses and pastry making.

2.3. Methods

2.3.1. Scanning Electronic Microscopy (SEM)

Scanning electronic microscopy (SEM) allows to produce high resolution images of the surface of a sample by using the principle of electron-matter interactions. An electron beam is projected onto the sample to be analyzed. The interaction between the electron beam and the sample generates low energy secondary

(a) (b)

Figure 5. (a) Powder of dried soil obtained from the sieve 0.4 mm, intended for the preparation of clay cakes, and (b) Dried clay cakes, consolidated by molasses, after a week of cure.

Table 2. Quantity of used materials [2].

	Quantity in masse to put into the mixer
Samples weight of dried ground	80 g
Water weight (/water = 15 wi)	50.4 g
0% of molasses	No molasses
4% of molasses	3.2 g
8% of molasses	6.4 g
12% of molasses	9.6 g
16% of molasses	12.8 g

electrons that are accelerated towards a secondary electron detector that amplifies the signal. Each point of impact corresponds to an electrical signal. The intensity of this electrical signal depends both on the nature of the sample at the point of impact, which determines the yield of secondary electrons, and on the topography of the sample at the point considered. It is thus possible, by scanning the beam over the sample, to obtain a map of the scanned area [3] [4].

2.3.2. N_2 Gas Adsorption Technique to Measure Pore Structure and Specific Surface Area

The experiments were conducted on a Micromeritics ASAP 2460 Version 2.01 instrument.

1) Procedure

One to three grams of sample is degassed at 200˚C for 24 hours under vacuum (<10 m Hg) prior to analysis, until the sample degassing rate is <0.005 Torr/min over a 15-minute interval. After this procedure, the tube and sample are weighted to determine the analytical weight of the test. The sample tube is then placed on the instrument's analysis port and the adsorption/desorption isotherms are collected. The resulting data is processed using several models depending on the desired result [12] [13] [14].

2) Barrett-Joyner-Halenda (BJH) method

The Barrett-Joyner-Halenda method is a procedure for calculating pore size distributions from experimental isotherms using the Kelvin pore filling model. It is applicable only to the mesopore and small macropore size range. The BJH method covers the mesopore range (>2 nm) [12] [13] [14].

3) Boer's t-Plot method

This method is most often used to determine the external surface area and micropore volume of microporous materials. It is based on standard isotherms and thickness curves that describe the statistical thickness of the adsorbent film on a non-porous reference surface [12] [13] [14].

4) Horvath-Kawazoe technique

This method provides a means by which the volume distribution of micropores by size is extracted from the experimental isotherm. The original H-K method is based on slit-shaped pores, but the additions by Saito-Foley and Cheng-Yang extend the method to be applied to cylindrical and spherical pores respectively [12] [13] [14] [15].

5) Dollimore Heal (DH) Method

Determination of the specific surface [12].

6) BET method

The Brunauer, Emmet and Teller method is used to determine the surface area on an adsorption model that incorporates multilayer coverage. The BET technique takes into account all accessible porosity within the grains themselves [12] [16].

3. Results and Discussion

3.1. Analysis by Electronic Microscopy of Scanning

3.1.1. Micrograph of Consolidated Soil at 0% of Sugar Cane Molasses

We observe a microstructure relatively less dense constituted of individualized aggregate piles and of aggregates in leaves of individualized clay, from this appears many inter-aggregate empties in the sample structure (**Figure 6(c)** and **Figure 6(d)**), in relation to the samples (**Figure 6(a)** and **Figure 6(b)**). We can distinguish piles of kaolinite minerals in plate form, that is piled one another (crystals are placed face to face) to constitute piles (**Figure 6(d)**). The soil being reserved, we observe a microstructure in separated aggregates, an opened texture and disorganization kaolin. Therefore, we observe a microstructure of matrix and clayey type as it is constituted of disorganized arrangement of kaolinite leaves between them.

3.1.2. Micrograph of Consolidated Soil at 8% of Sugar Cane Molasses

At 10 μm (**Figure 7(a)**) we observe the making of aggregate piles, the aggregates of the individualized leaves organize in piles at 1 μm (**Figure 7(d)**) and 2 μm (**Figure 7(c)**) aggregates piles similar to various and deep macro pores. However,

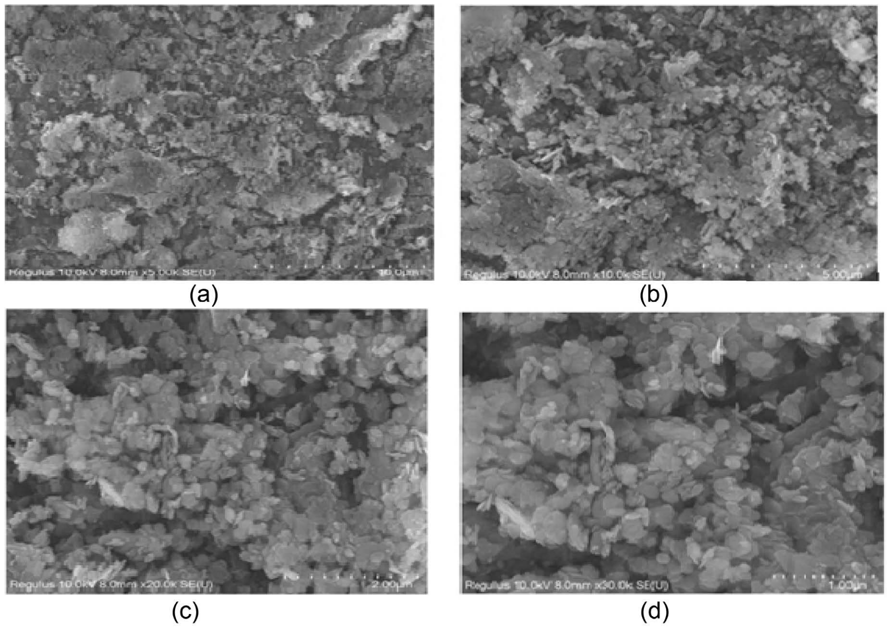

Figure 6. Micrograph of raw briquette sample without sugar cane molasses (0%) (a) at 10 μm, (b) at 5 μm, (c) at 2 μm, (d) at 1 μm.

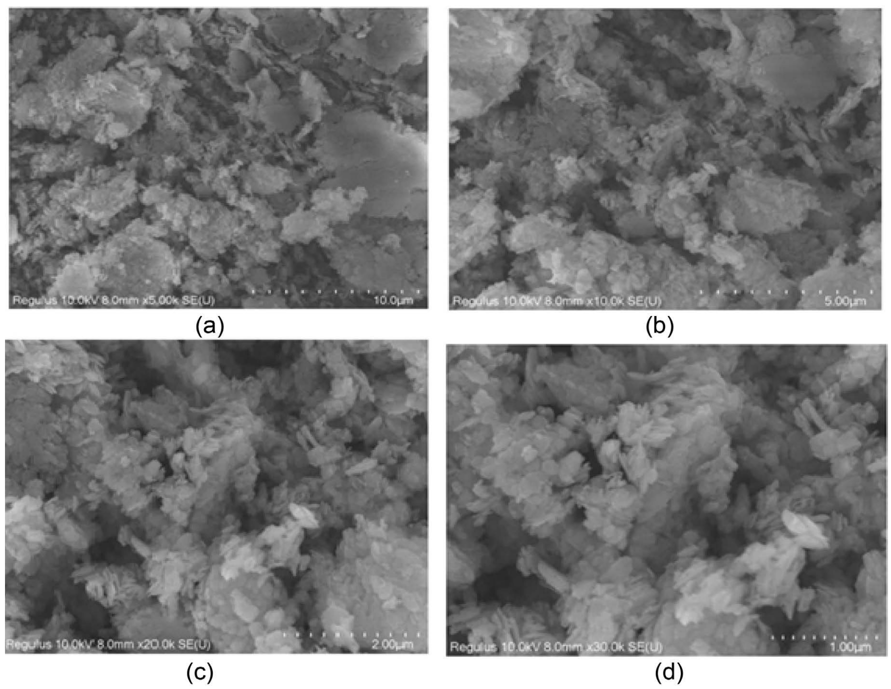

Figure 7. Micrograph of consolidated raw briquette sample at 8% of sugar cane molasses (a) at 10 μm, (b) at 5 μm, (c) at 2 μm, (d) at 1 μm.

we can observe a reduction of the porosity compared with those observed on consolidated sample at 0%.

3.1.3. SEM Micrograph of Soil Stabilized with 12% Sugarcane Molasses

At 10 μm (**Figure 8(a)**) we observe the presence of aggregate piles, more than

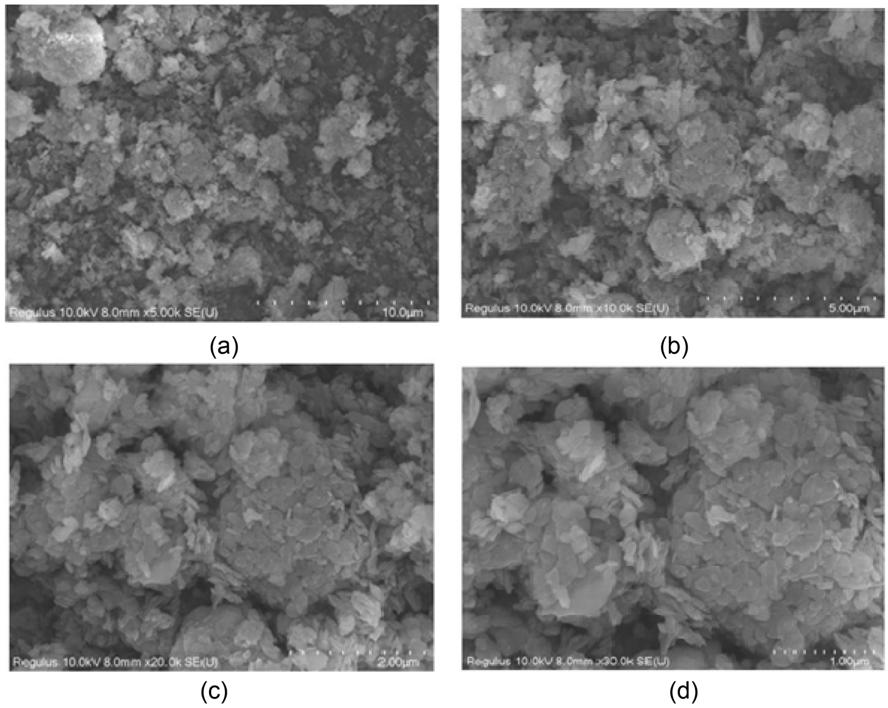

Figure 8. Micrograph of consolidated raw briquette sample at 12% of sugar cane molasses (a) at 10 μm, (b) at 5 μm, (c) at 2 μm, (d) at 1 μm.

for the consolidated sample at 8% and 0% of sugar cane molasses, at 1 μm (**Figure 8(d)**) and at 2 μm (**Figure 8(c)**) aggregate piles are well visible with the presence of inter-aggregate empties too few and little deep compared with those observed on consolidated sample at 8%, 0% of sugar cane molasses.

3.1.4. Micrograph of Consolidated Soil at 16% of Sugar Cane Molasses

At 10 μm (**Figure 8(a)**), we observe the presence of aggregate masses, more numerous than for sample at 8% and 1 μm (**Figure 9(d)**) and 2 μm (**Figure 9(c)**) aggregate masses are well visible with the presence of inter aggregate empties little numerous and deep as if they discovered and compared with those observed from consolidated sample at 0%, 8%, 12%.

We observe the evolution of the soil microstructure of a structure little dense constituted with individualized aggregate masses and individualized aggregate leaves, with many inter-aggregate empties (micro pores) (sample at 0%), that is, a clayey matrix microstructure to an aggregated structure or individualized aggregate masses and aggregates in individualized leaves gather to constitute bigger aggregate masses and more linked to reduced micro porosity (consolidated sample at 8%, 12%, and 16%). Sugar cane molasses behaves like a linking in the soil matrix putting together aggregates of clay leaves one another. But, we observe the presence of inter-aggregate pores (mesopores) of similar size in all samples. Jijo James (2020), studying the effects of PM on the microstructure of LSS (lime-stabilized soil (LSS)), shows that the soil particles aggregated to form floks, and pozzolanic reactions resulted in an aggregated mass density responsible

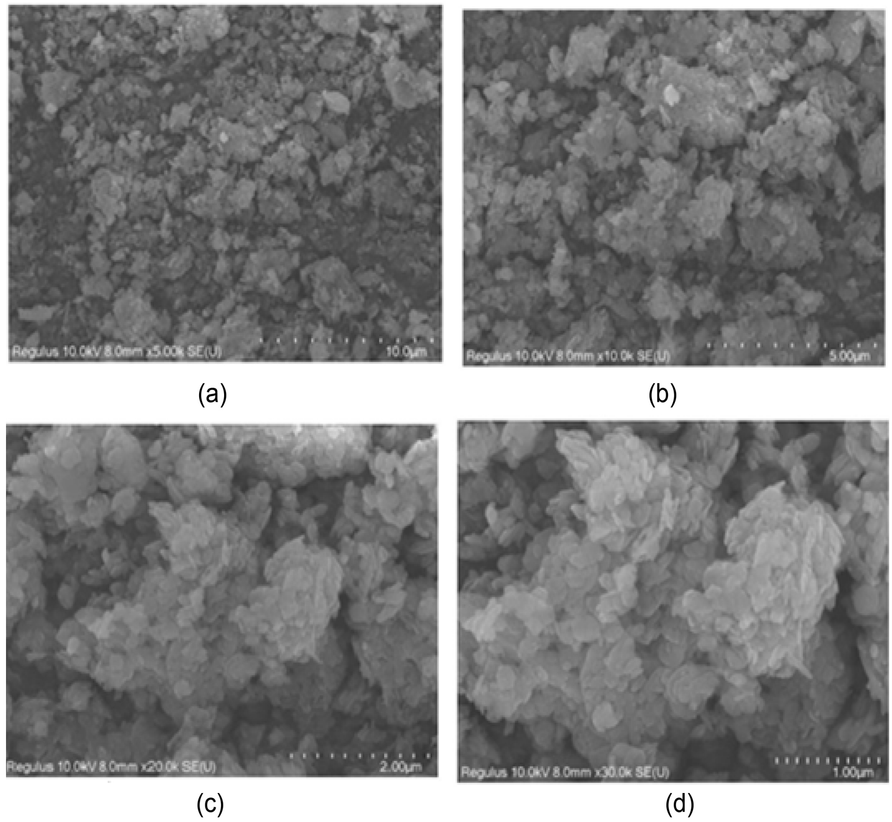

Figure 9. Micrograph of consolidated raw briquette sample at 16% of sugar cane molasses (a) at 10 μm, (b) at 5 μm, (c) at 2 μm, (d) at 1 μm.

for the strength gain. Individual clay platelets are not visible after lime addition, since the grain structure was destroyed and new reaction products are formed with the process of pozzolanic reactions [17]. Muhmed and Wanatowski (2013) also reported that soil particles aggregated to form clusters due to lime treatment of kaolin clay [18]. Al-Mukhtar *et al.* (2012) also reported the formation of a dense compact mass due to the stabilization of expansive soil with lime [19]. Millogo Y. (2008), examining the effect of adding cement to lateritic gravels, finds the presence of isolated particles of quartz and kaolinite in the raw sample. The addition of cement leads to the formation of particle agglomerates resulting from flocculation and the increase in particle size of the raw sample with the addition of cement [20]. Thanh D (2014) shows that the microstructure of the lime treated soil and the untreated soil are totally different. For the untreated sample, a compacted aggregate structure formed by the clay particles and inter-aggregate pores can be observed. For the sample treated with lime, after saturation, a compacted aggregate and granular structure with new hydrates were observed [3]. EL Fgaier Faycal (2013) finds that the Leers soil sample has an open texture with no preferential arrangement of the laminae. The random orientation reveals voids in the sample structure, and subsequently the appearance of a network of discontinuities [21].

3.2. Porosity and Specific Surface by Brunauer, Emmet, and Teller (B.E.T)

The desorption takes place in more stable conditions. Thus, the isothermal of desorption is used for the analysis of the porosity, the distribution of pore size is measured by isothermal of nitrogen desorption. The specific surface is obtained by B.E.T [12] [13] [14].

3.2.1. Results of Porosimetrical Testing by BJH Method on Soil without Sugar Cane Molasses (0%)

Figure 10 shows that the accumulated porous volume is 0.055 cm^3/g (**Figure 10(a)**). The distribution curve of pore diameters (**Figure 10(b)** and **Figure 10(c)**) shows that the sample without sugar cane molasses (0%) presents a trimodal distribution with three families of mesopores: A mesopore family centered towards 5.2 nm, a mesopore family centered towards 7 nm and a centered mesopores and a mesopore family centered towards 12.5 nm.

3.2.2. Results of Porosimetric Testing by BJH Method of Consolidated Soil at 8% of Sugar Cane Molasses

Figure 11 shows that the accumulated porous volume is 0.036 cm^3/g (**Figure 11(a)**). The distribution curve of pore diameters (**Figure 11(b)** and **Figure 11(c)**) shows that the consolidated sample at 8% of sugar cane molasses presents a mono modal distribution of centered mesopores towards 9 nm.

3.2.3. Results of Porosimetrical Tests by BJH Method on Consolidated Soil at 12% of Sugar Cane Molasses

Figure 12 shows that the accumulated porous volume is 0.017 cm^3/g (**Figure 12(a)**). The distribution curve of pore diameters (**Figure 12(b)** and **Figure 12(c)**) shows that consolidated sample at 12% of sugar cane molasses presents a mono modal centered distribution towards 12.5 nm.

3.2.4. Results of Porosimetric Tests by the BJH Method of the Soil Stabilized with 16% Sugar Cane Molasses

Figure 13 shows that the accumulated porous volume is 0.090 cm^3/g (**Figure 13(a)**). The distribution curve of pore diameters (**Figure 13(b)** and **Figure 13(c)**) shows that the consolidated sample at 16% of sugar cane molasses presents a bimodal centered distribution towards 12.5 nm and 15 nm.

Accumulated mesoporous volume of samples is reduced with the increasing of sugar cane molasses quantity. The sample without sugar cane molasses (0%) has the highest accumulated mesoporous volume 0.055 cm^3/g, followed by the consolidated sample at 8% of sugar cane molasses 0.036 cm^3/g, then by consolidated sample at 12% of sugar cane molasses 0.017 cm^3/g, finally consolidated sample at 16% of sugar cane molasses an accumulated mesoporous volume 0.037 cm^3/g.

We find the same family of mesopores (2 nm < d < 50 nm) dominating, centered towards 12.5 nm, in all samples. There is the presence of centered mesopore family towards 5.2 nm and 7 nm on the sample without sugar cane molasses (0%). Those mesopore families disappear in consolidated samples at 8%,

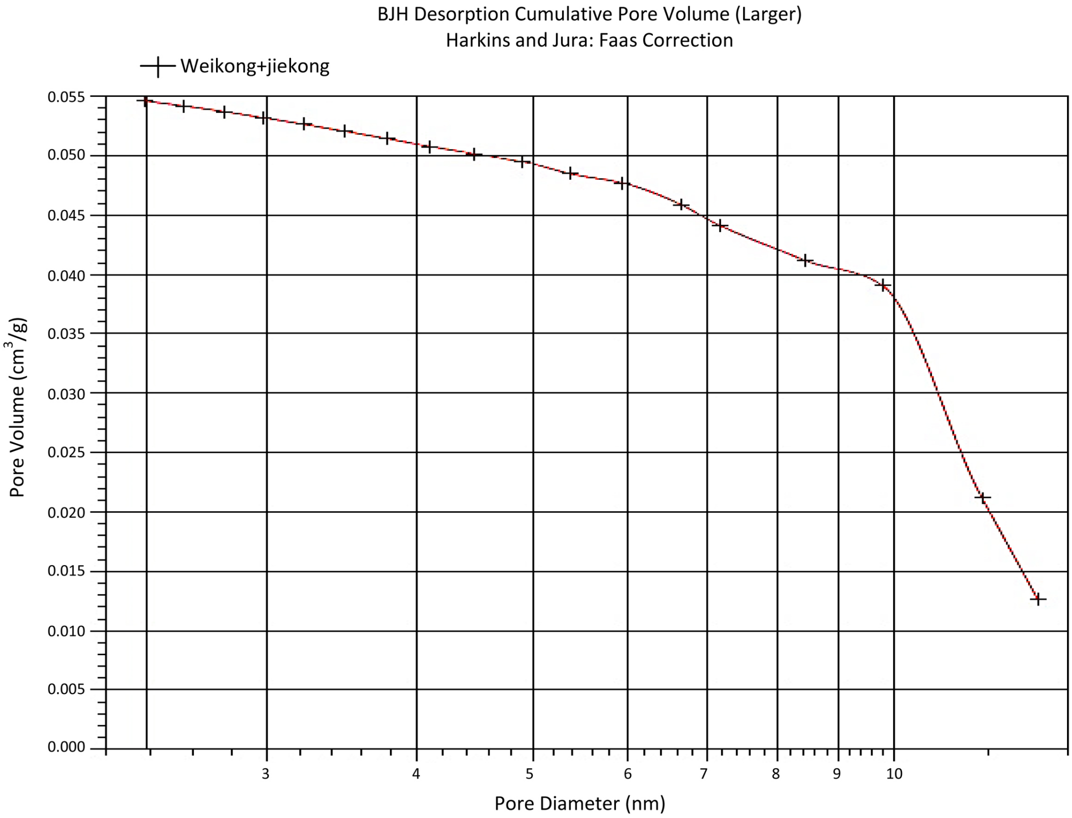
BJH Desorption Cumulative Pore Volume (Larger)
Harkins and Jura: Faas Correction
Weikong+jiekong
Pore Volume (cm³/g)
0.055
0.050
0.045
0.040
0.035
0.030
0.025
0.020
0.015
0.010
0.005
0.000
3
4
5
6
7
8
9
10
Pore Diameter (nm)
(a)

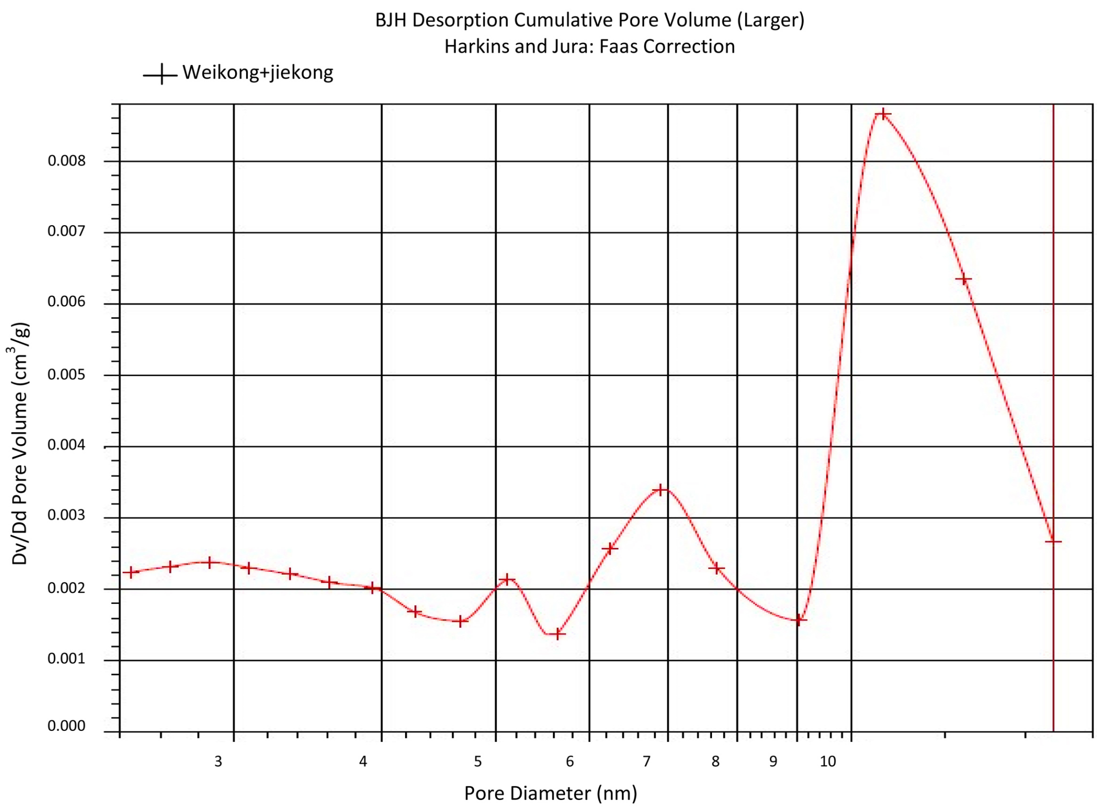
BJH Desorption Cumulative Pore Volume (Larger)
Harkins and Jura: Faas Correction
Weikong+jiekong
Dv/Dd Pore Volume (cm³/g)
0.008
0.007
0.006
0.005
0.004
0.003
0.002
0.001
0.000
3
4
5
6
7
8
9
10
Pore Diameter (nm)
(b)

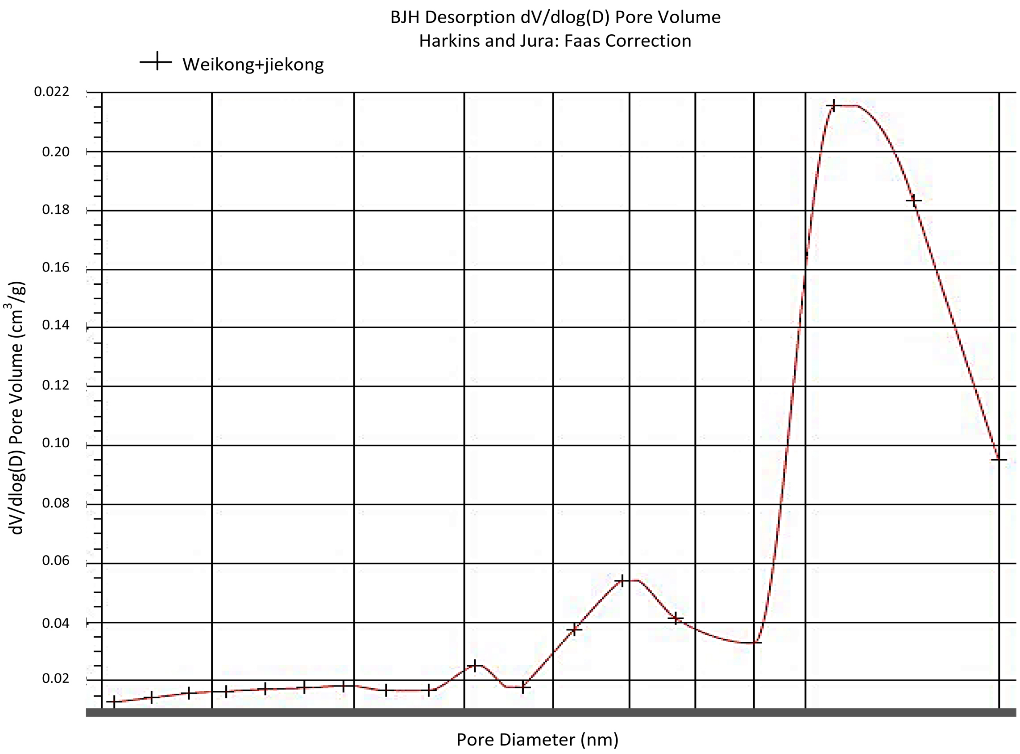

(c)

Figure 10. Sample without sugarcane molasses (0%). (a) Accumulated curves (in volume) of distribution of sample pores; (b) Derived curve of distribution of pore access diameters; (c) Logarithmic derived curve of pore distribution.

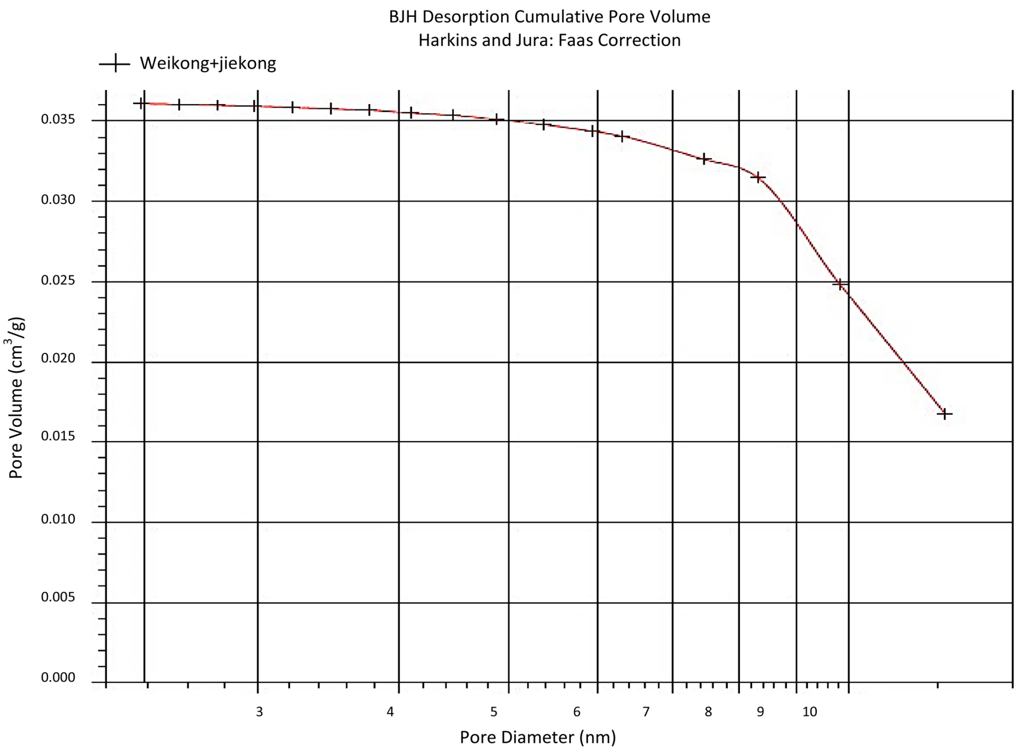

(a)

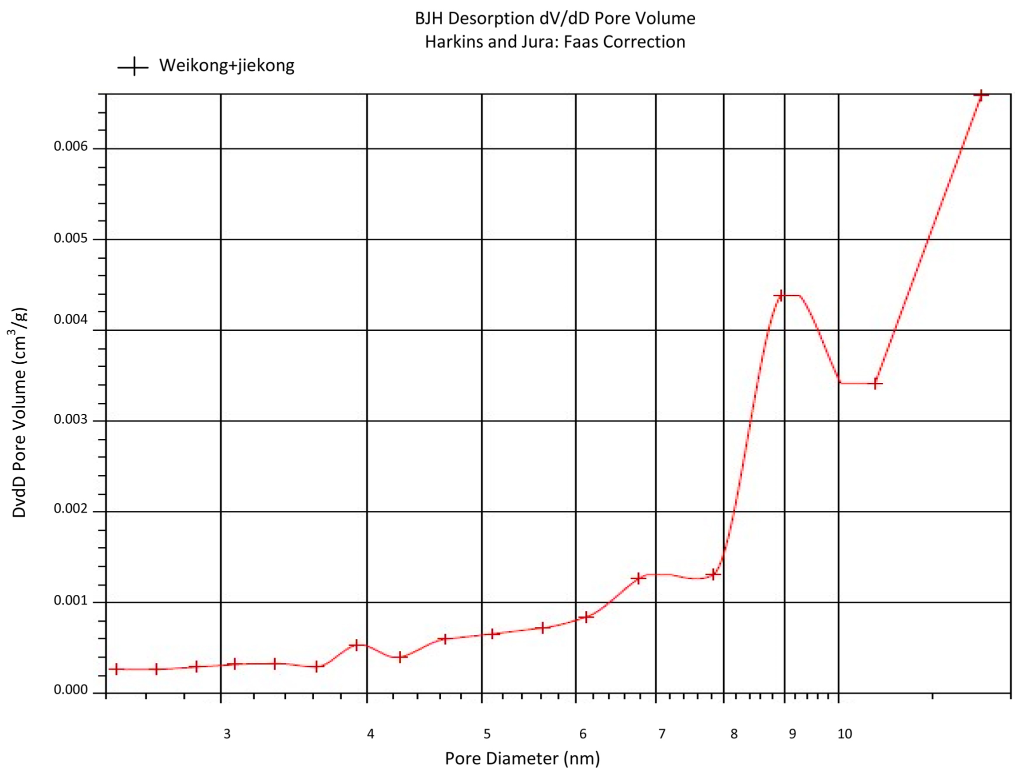

(b)

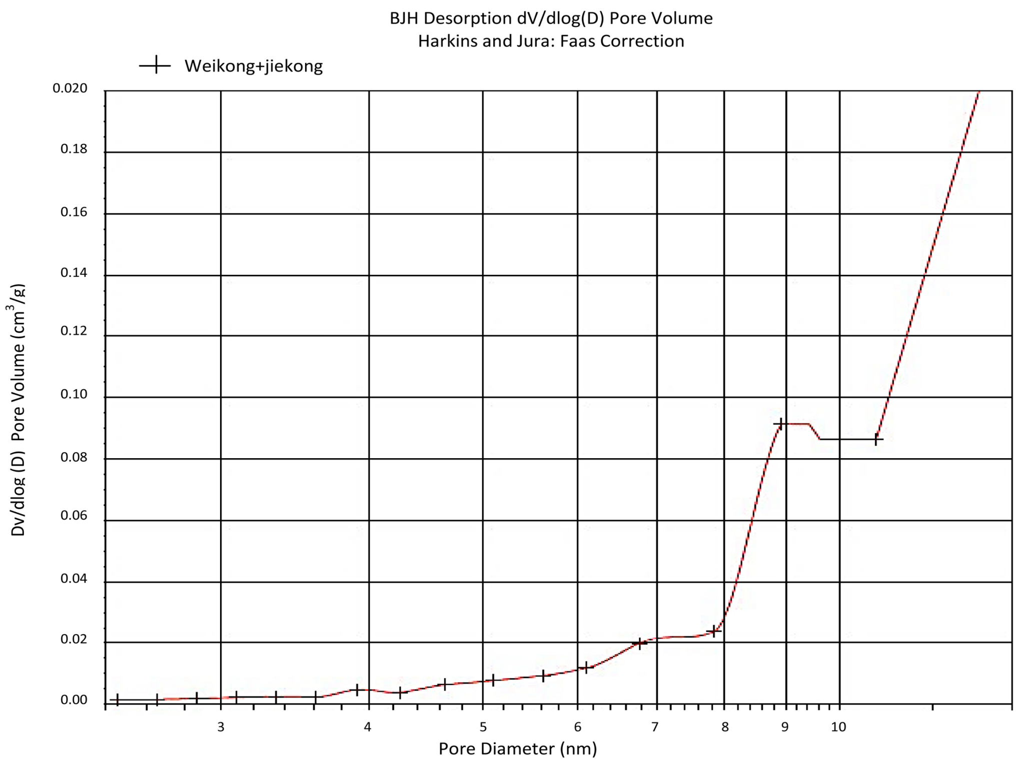

(c)

Figure 11. Consolidated sample at 8% of sugar cane molasses. (a) Accumulated curves (in volume) of pore distribution; (b) Distribution derived curve of pore access diameters; (c) Logarithmical derived curve of pore distribution.

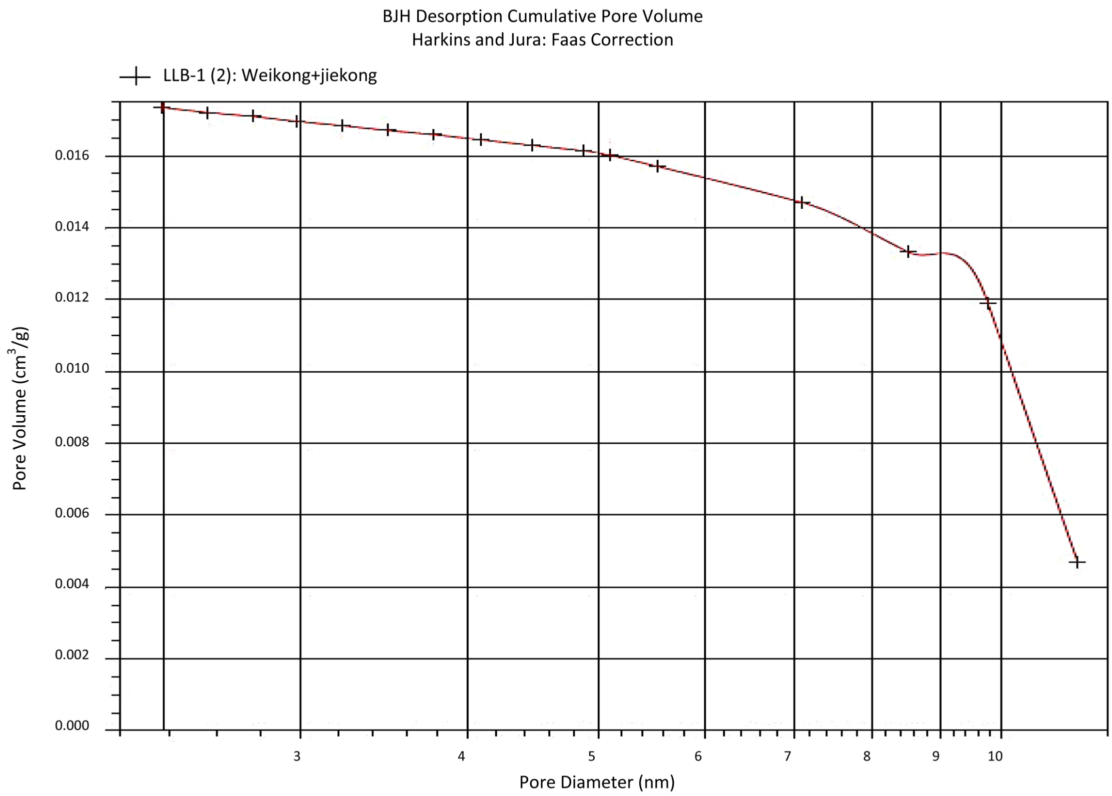
BJH Desorption Cumulative Pore Volume
Harkins and Jura: Faas Correction
LLB-1 (2): Weikong+jiekong
Pore Volume (cm³/g)
0.016
0.014
0.012
0.010
0.008
0.006
0.004
0.002
0.000
3
4
5
6
7
8
9
10
Pore Diameter (nm)

(a)

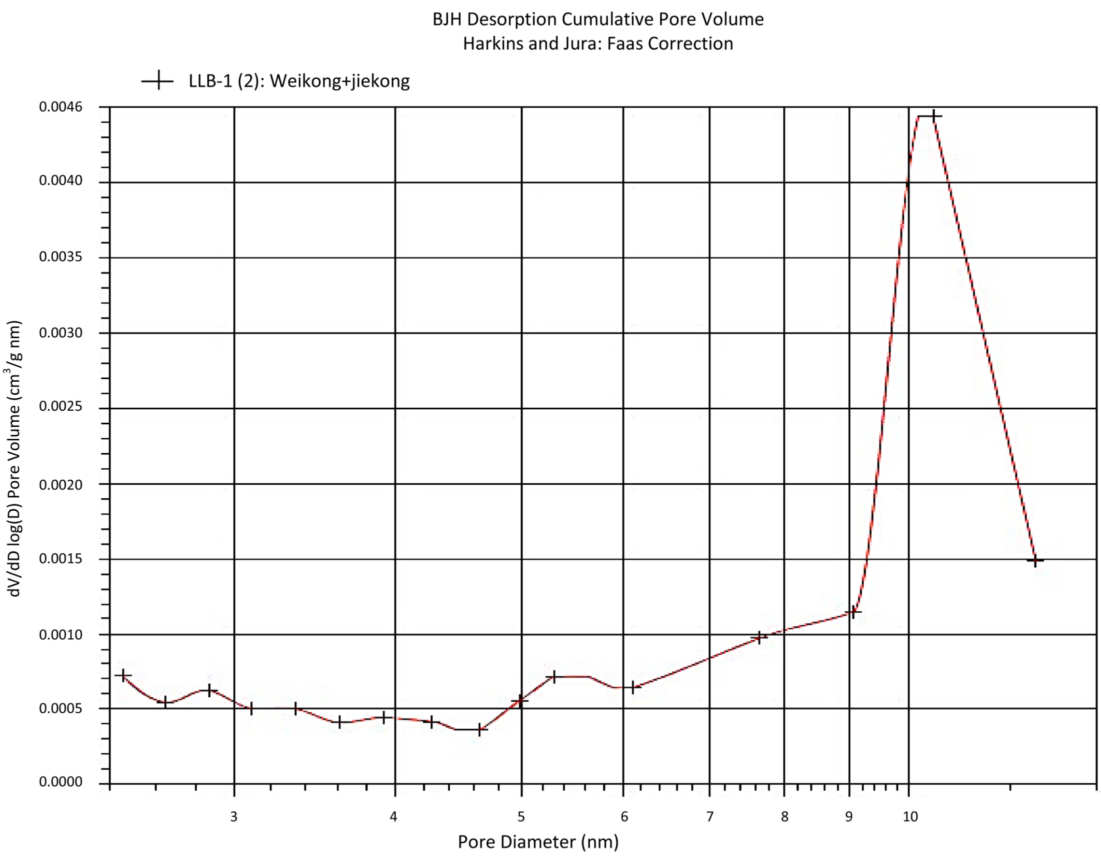
BJH Desorption Cumulative Pore Volume
Harkins and Jura: Faas Correction
LLB-1 (2): Weikong+jiekong
dV/dD log(D) Pore Volume (cm³/g nm)
0.0046
0.0040
0.0035
0.0030
0.0025
0.0020
0.0015
0.0010
0.0005
0.0000
3
4
5
6
7
8
9
10
Pore Diameter (nm)

(b)

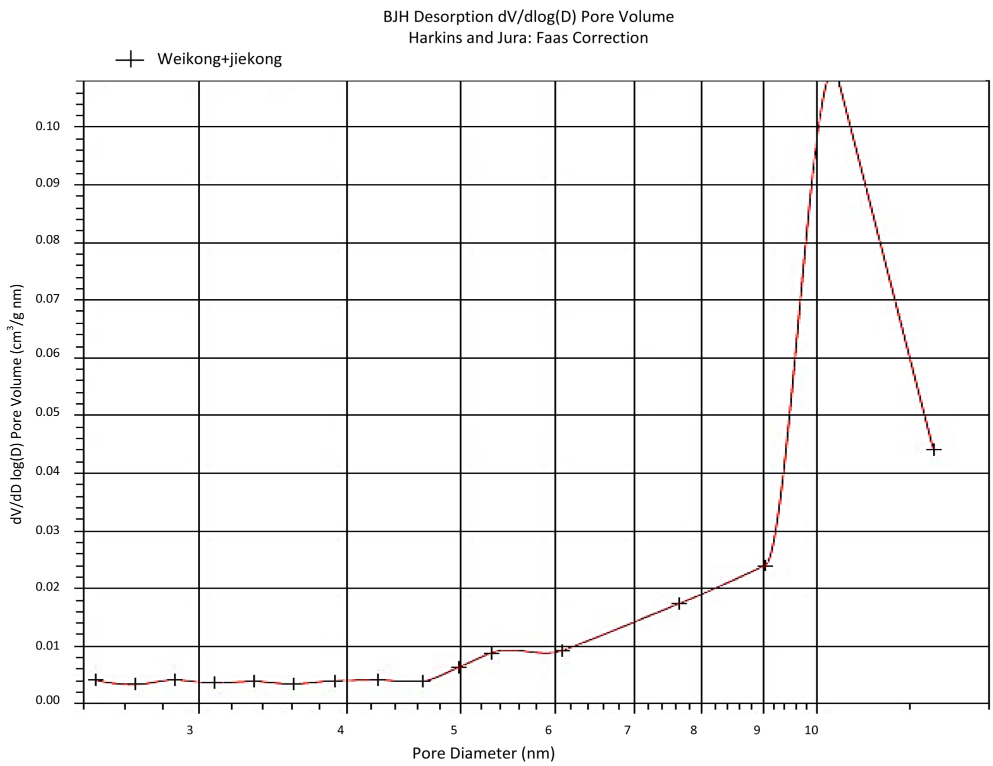

(c)

Figure 12. Consolidated sample at 12% of sugar cane molasses. (a) Accumulated curves (in volume) of pore distribution; (b) Distribution derived curve of pore access diameters; (c) Logarithmical derived curve of pore distribution.

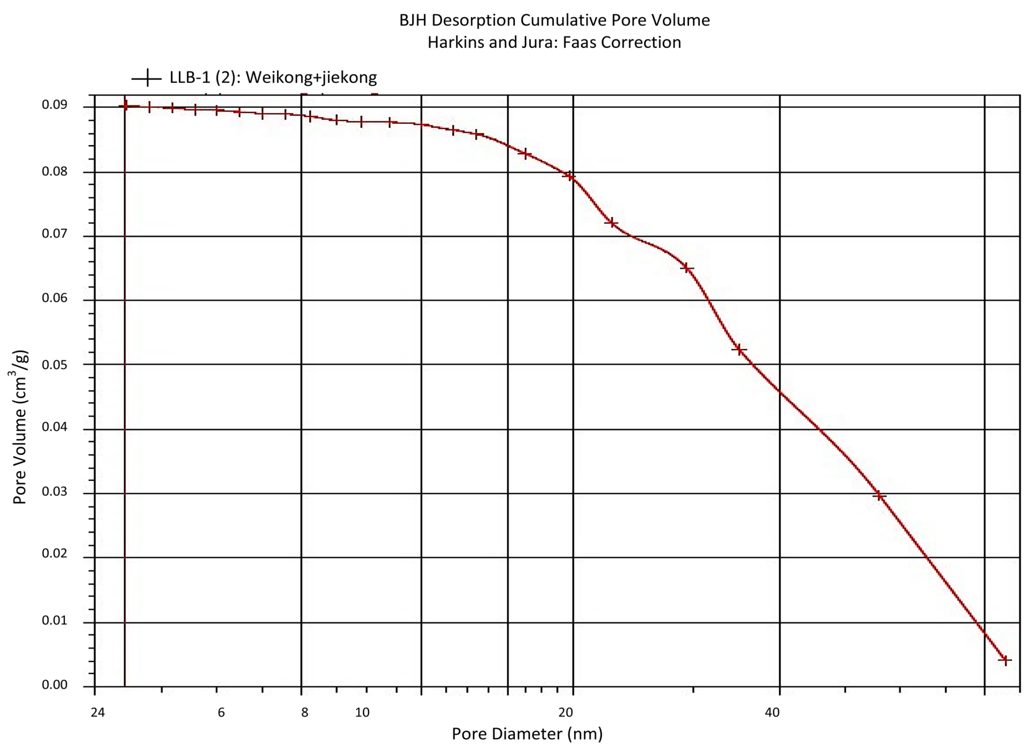

(a)

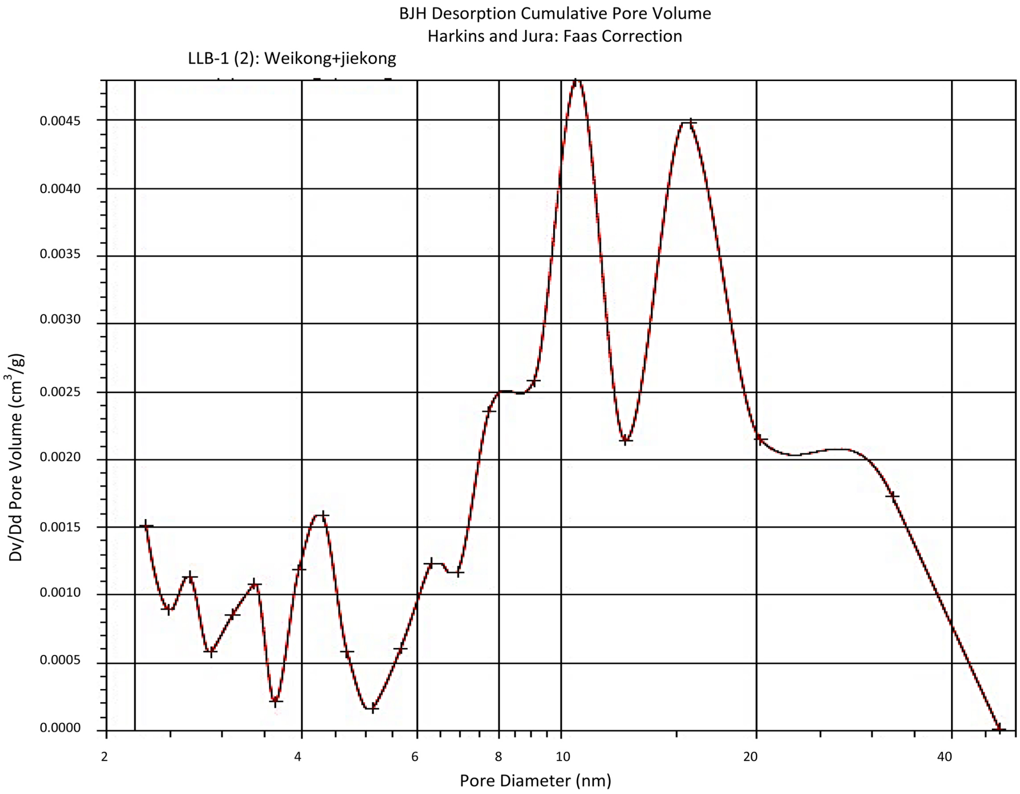

(b)

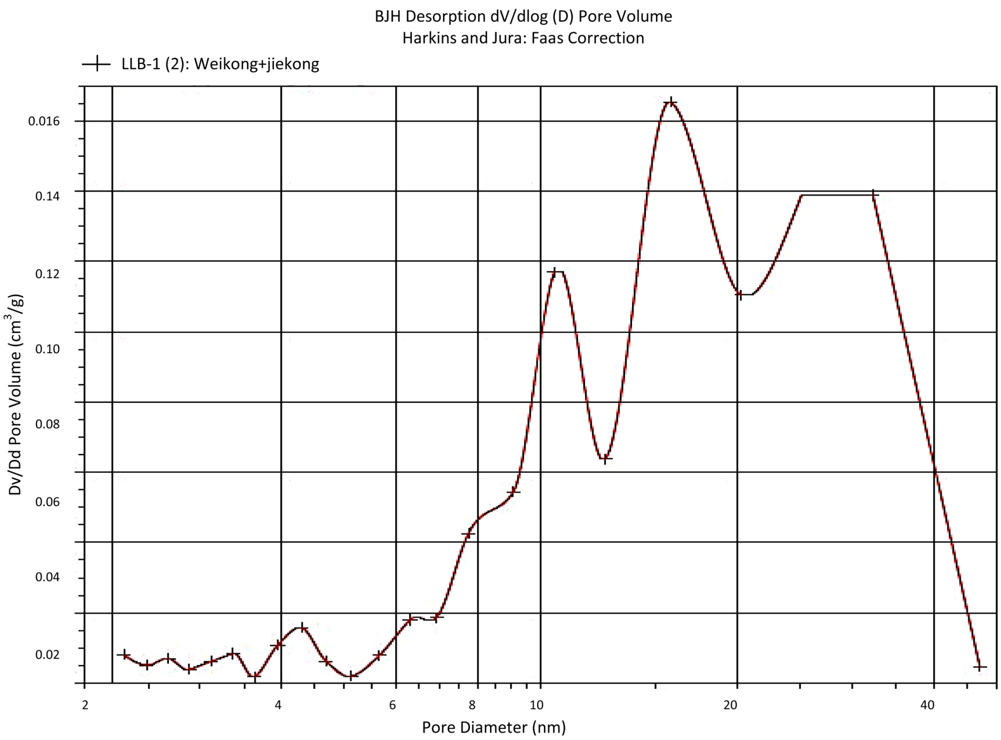

(c)

Figure 13. Consolidated sample at 16% of sugar cane molasses. (a) Accumulated curves (in volume) of pore distribution; (b) Distribution derived curve of pore access diameters; (c) Logarithmical derived curve of pore distribution.

Table 3. Pore volumes obtained by the BJH method.

	BJH		t-Plot	Horvath Kawazoe
	cumulative Pore Volume$_{adsorption}$ (cm^3/g)	Cumulative Pore Volume$_{désorption}$ (cm^3/g)	Micropore volume (cm^3/g)	Maximum pore volume at Relative Pressure: 0.154961545 (cm^3/g)
0% sugar cane molasses	0.049999	0.054612	0.000963	0.013461
8 % sugar cane molasses	0.028453	0.036088	0.001665	0.008816
12% sugar cane molasses	0.026817	0.017345	0.000660	0.007584
16% sugar cane molasses	0.02205	0.037689	−0.000729	0.009236

12%, and 16%. The sugar cane molasses seems to have little effect on the mesopore size (>9 nm) in these materials. It acts on the pore size (<9 nm) by occupying them.

Micro porous volumes of samples are also reduced with the increase of sugar cane molasses quantity. The sample without sugar cane molasses (0%) has the highest micro porous volume 0.000963 cm^3/g, followed by consolidated sample at 8% of sugar cane molasses 0.001665 cm^3/g, then by consolidated sample at 12% of sugar cane molasses 0.000660 cm^3/g, finally by consolidated sample at 16% of sugar cane molasses −0.000729 cm^3/g.

The reduction of mesoporous volume according to the increasing of quantity of sugar cane molasses in the material suggests that organic constituents of sugar cane molasses occupy mesopores superimposed coats between piles of particular clay, without saturating mesopores > 9 nm in which there are physical interactions of weak intensity. So, there is a reduction of accessible mesoporous volume without modifying the size of mesopores 12.5 nm (**Table 3**).

The decrease of the microporous volume according to the increase in the amount of sugarcane molasses in the material suggests that the organic constituents of the sugarcane molasses occupy the micropores through the film of absorbed water condensed as a meniscus between the clay particles until they fill them up. This is the place of high-intensity physical interactions. Indeed, the size of a micropore being very small (<2 nm), a single gas molecule occupies the pore and leads to the reduction of the size and the filling of the pore. In micropores, there is no layer formation [11] [12].

The decrease of porous volume (micro pores and mesopores) and of the specific area with the quantity of sugar cane molasses suggest the evolution of soil structure towards more dense and compact structure [17] [22] [23]. Consequently, consolidated samples at 8%, 12% and 16% will have superior mechanical properties to the sample without sugar cane molasses (0%). As a result, samples stabilized at 8%, 12% and 16% will have superior mechanical properties to the sample without sugarcane molasses (0%). Ashori A. *et al.* (2012) found that sucrose, the main constituent of sugarcane molasses penetrated pores > 0.8 nm. Sucrose migrates with the adsorbed water and forms a crust on the paper surface [24]. According to Utpalendu Kuila (2013), the organic matter (OM) present in earthen concretes occupies the mesopores in the earthen blocks [14].

Siti Aisyah *et al.* (2020), when studying the effect of porosity and water absorption on compressive strength, finds that the fly ash-based geopolymer with lower porosity has the high compressive strength while the OPC with higher porosity has lower compressive strength [22].

3.2.5. Specific Area of Consolidated Soil with Sugar Cane Molasses

The obtained specific areas with BET method, BJH method, and D-H method are given in **Table 4**.

The sample without sugar cane molasses possesses the highest specific area S(BET) = 32.8433 cm^2/g, S(BJH) = 24.206 cm^2/g, S(D-H) = 29.011 cm^2/g. Then, the consolidated sample at 8% of sugar cane molasses S(BET) = 21.0425 cm^2/g, S(BJH) = 12.058 cm^2/g and S(D-H) = 16.739 cm^2/g. After the consolidated sample at 12% of sugar cane molasses, S(BET) = 18.6091 cm^2/g, S(BJH) = 12.015 cm^2/g and S(D-H) = 15.908 cm^2/g, for consolidated sample at 16% of sugar cane molasses S(BET) = 23.5626 cm^2/g, S(BJH) = 22.1488 cm^2/g and S(D-H) = 22.5394 cm^2/g.

Whatever method, the sample without sugar cane molasses possesses the highest specific area.

The specific area is reduced with the increase of the sugar cane molasses quantity in the ground. The sugar cane molasses contains molecules that occupy the external specific area of clay soil.

Table 4. Obtained specific areas with BET method, BJH method, and D-H method.

	BJH		D-H		t-Plot	BET
	Cumulative surface area of $pores_{adsorption}$ (m^2/g)	Cumulative surface area of $pores_{désorption}$ (m^2/g)	Cumulative surface area of $pores_{adsorption}$ (m^2/g)	Cumulative surface area of $pores_{désorption}$ (m^2/g)	Micropore Area (m^2/g)	Surface Area (BET) (m^2/g)
0% sugar cane molasses	24.206	24.9641	29.011	31.4760	1.8150	32.8433
8 % sugar cane molasses	12.058	14.3269	16.739	18.6528	3.5547	21.0425
12% sugar cane molasses	12.015	8.0493	15.908	17.5894	1.6426	18.6091
16% sugar cane molasses	11.58	15.135	22.5394	23.9915	-	23.5626

The results obtained corroborate with some results obtained by other researchers.

Saiyouri (1996) notes that the presence of non-clay elements significantly reduces the specific surface of a clayey [25]. Errais Emna (2011), when studying the adsorption of anionic dyes on clays, notes that the specific surface area of clays decreases significantly after the adsorption of dye molecules, regardless of the clay. This means that the surface accessible to adsorption has decreased. Indeed, the SEM images showed that the aggregates of particles were covered by a compact film and a porosity, which were no longer visible. The dye molecules had completely filled the inter-aggregate spaces, which would have reduced the adsorption surfaces and thus the specific surface [26]. Ikram Jarraya *et al.* (2010), when studying the adsorption of VOC (volatile organic compounds) by a Tunisian organo-modified clay material, noticed that the BET specific surface of natural clay material had strongly decreased after intercalation. These observations supported the idea that the access of nitrogen to the surface is blocked by the covalent organic moieties bound to the edges of the OH groups of the clay sheets, hence the reduction of the microporous contribution due to the occupation or blocking of some pores by the intercalating agent [27]. Sebei Haroun (2013), studied the interactions of inorganic and organic pollutants with phosphocalcic matrices, he notes that the specific surface area and pore volume decrease when increasing the amount of zinc fixed in the Ca-HA-P matrix (phosphocalcic powder). This may correspond to an increase in the number of reactive sites occupied by zinc in the Ca-HAP porosity, suggesting intraparticle diffusion mechanisms [28].

4. Conclusions

The electronic microscopy of sweeping has allowed us to make a quantitative study of microstructure. The nitrogen adsorption has allowed us to make a qualitative study of the microstructure.

The isotherms of nitrogen adsorption and the specific area are determined by BET method, the volume of micropores is obtained by t-plot method, and the volume of mesopores is obtained by BJH method on the space of 2.3034 nm and 29.8817 nm of diameter. The obtained results have allowed us to notice that:

1) Sugar cane molasses acts on the structure of fine clayey soil by developing its microstructure of a microstructure of ventilated matrix type (sample without sugar cane molasses (0%) to a microstructure of more compact aggregated (consolidated sample at 8%, 12%, 16% of sugar cane molasses).

2) Sugar cane molasses acts on the porous volume (micropore < 2 nm and mesopore < 9 nm) by reducing it which means the sugar cane molasses occupies the porous volume of sample. However, it seems to have no effect on the size of mesopores > 9 nm.

3) sugar cane molasses reduces the specific area of clay soil. That means sugar cane molasses contains molecules that occupy the external specific surface of the

soil clayey.

4) Sugar cane molasses induce the evolution of the soil structure towards more dense and compact structure. Consequently, the consolidated materials with sugar cane molasses will have superior mechanical properties against those ones materials consolidated soil without molasses (0%).

Acknowledgements

We are deeply thankful to DuongLab, Department of Chemistry, Biochemistry and Physics and Hydrogen Research Institute, Université du Québec à Trois-Rivières, Trois-Rivières, Québec, G9A5H7, *Canada* for facilities.

We would like to thank Mr. Nakoupakou, a certified English teacher at Nkayi High School for constructive discussion.

Conflicts of Interest

The authors declare no conflicts of interest regarding the publication of this paper.

References

[1] Narcisse, M., Louzolo-Kimbembe, P. and Tamba-Nsemi, Y.D. (2017) Etude des caractéristiques mécaniques d'une brique en terre stabilisée à l'aide de la mélasse de canne à sucre. *Revue du CAMES—Sciences Appliquées et de l'ingénieur Cames*, **2**, 1-9. http://publication.lecames.org

[2] Ngouallat, M.N., Malanda, N. and Louzolo-Kimbembe, P. (2020) Analyse macroscopique des effets de la mélasse de canne à sucre sur le sol fin argileux. *Revue RAMReS—Sciences appliquées et de l'ingénieur*, **2**, 24-31.

[3] Tran, T.D. (2014) Rôle de la microstructure des sols argileux dans les processus de retrait-gonflement: De l'échelle d'éprouvette à l'échelle de la chambre environnementale. Thèse de l'école nationale supérieure des mines de paris, spécialité: Géologie de l'ingénieur.

[4] Maison, T. (2011) Analyse à l'échelle microscopique des phénomènes d'humectation et de dessiccation des argiles. Thèse de l'école centrale des arts et manufactures, école centrale paris.

[5] Gloria, R., Macías, C., Haro, M., Jagiello, J. and Ania, C.O. (2015) Effects of CO_2 Activation of Carbon Aerogels Leading to Ultrahigh Micro-Meso Porosity. *Microporous and Mesoporous Materials*, **209**, 18-22. https://doi.org/10.1016/j.micromeso.2015.01.011

[6] Rouquerol, F. (1965) Contribution à l'étude, par adsorption gazeuse, de la texture des solides divisés. Application à l'alumine, a la glucine et a différents gels et oxydes. Faculté des sciences de l'Université de Paris, Paris.

[7] Matthias, T., Kaneko, K., Neimark, A.V., Olivier, J.P., Rodriguez-Reinoso, F., Rouquerol, J. and Sing, K.S.W. (2014) Physisorption of Gases, with Special Reference to the Evaluation of Surface Area and Pore Size Distribution (IUPAC Technical Report). https://doi.org/10.1515/pac-2014-1117

[8] Le Phuong Thu (2013) Oxydation en voie humide des effluents des distilleries d'alcool à partir de canne à sucre en présence de catalyseurs Ru et Pt supportés sur TiO_2 ou ZrO_2 Catalyse. Thèse de l'Université Claude Bernard-Lyon I, Lyon.

[9] Belghiti-Alaoui, A. (1993) Nature des polysaccharides issus du process d'extraction du saccharose à partir de la betterave. Thèse de l'institut national de Lorraine, Spécialité Biotechnologie et Industries Alimentaires.

[10] Mathlouthi, M. (1998) bases de l'infrarouge à transformée de fourrier et applications aux sucres.

[11] Janekarn, I., Hunt, A.J., Ngernyen, Y., Youngme, S. and Supanchaiyamat, N. (2020) Graphitic Mesoporous Carbon-Silica Composites from Low Value Sugarcane By-Products for the Removal of Toxic Dyes from Wastewaters. *Royal Society Open Science*, **7**, Article ID: 200438. https://doi.org/10.1098/rsos.200438

[12] Klobesf, P., Klaus, M. and Mu, R.G. (2006) Porosity and Specific Surface Area Measurements for Solid Materials. Special Publication 960-17.

[13] Joewondo, N. (2018) Pore Structure of Micro- and Mesoporous Mudrocks Based on Nitrogen and Carbon Dioxide Sorption.

[14] Kuila, U. (2013) Measurement and Interpretation of Porosity and Pore-Size Distribution in Mudrocks: The Hole Story of Shales.

[15] Hussami, L. (2010) Synthesis, Characterization and Application of Multiscale Porous Materials. TRITA-CHE Report 2010.

[16] Brunauer, S., Emmett, P.H. and Teller, E. (1938) Adsorption of Gases in Multimolecular Layers. *Journal of the American Chemical Society*, **60**, 309-319. https://doi.org/10.1021/ja01269a023

[17] James, J. (2020) Sugarcane Press Mud Modification of Expansive Soil Stabilized at Optimum Lime Content: Strength, Mineralogy and Microstructural Investigation. *Journal of Rock Mechanics and Geotechnical Engineering*, **12**, 395-402. https://doi.org/10.1016/j.jrmge.2019.10.005

[18] Muhmed, A. and Wanatowski, D. (2013) Effect of Lime Stabilisation on the Strength and Microstructure of Clay. *IOSR Journal of Mechanical and Civil Engineering*, **6**, 87-94. https://doi.org/10.9790/1684-638794

[19] Al-Mukhtar, M., Khattab, S. and Alcover, J. (2012) Microstructure and Geotechnical Properties of Lime-Treated Expansive Clayey Soil. *Engineering Geology*, **139-140**, 17-27. https://doi.org/10.1016/j.enggeo.2012.04.004

[20] Millogo, Y. (2008) Etude géotechnique, chimique et minéralogique de matières premières argileuse et latéritique du Burkina Faso améliorées aux liants hydrauliques: Application au génie civil (bâtiment et route). Thèse de l'université de ouagadougou.

[21] El Fgaier, F. (2013) Conception, production et qualification des briques en terre cuite et en terre crue. Thèse de doctorat délivrée par l'école centrale de Lille. https://tel.archivesouvertes.fr/tel-01242549/document

[22] Razak, A.S., Zainal, F.F. and Shamsudin, S.R. (2020) Effect of Porosity and Water Absorption on Compressive Strength of Fly Ash Based Geopolymer and OPC Paste. *IOP Conference Series: Materials Science and Engineering*, **957**, Article ID: 012035. https://doi.org/10.1088/1757-899X/957/1/012035

[23] Yibas, M., Quezon, E.T. and Geremew, A. (2018) Combined Effects of Molasses-Lime Treatment on Poor Quality Natural Gravel Materials Used for Sub-Base and Base Course Construction. *GSJ*, **6**, 621-633.

[24] Alireza, A., Marashi, M., Ghasemian, A. and Afra, E. (2012) Utilization of Sugarcane Molasses as a Dry-Strength Additive for Old Corrugated Container Recycled Paper. *Composites Part B: Engineering*, **45**, 1595-1600. https://doi.org/10.1016/j.compositesb.2012.09.030

[25] Saiyouri, N. (1996) Approche microstructurale et modélisation des transferts d'eau et du gonflement dans les argiles non saturées. Thèse doctorat, Ecole Centrale Paris, Paris, 228 p.

[26] Errais, E. (2011) Réactivité de surface d'argiles naturelles. Étude de l'adsorption de colorants anionique. Thèse de doctorat de l'Université de Strasbourg, Strasbourg.

[27] Jarraya, I., Fourmentin, S. and Benzina, M. (2010) Adsorption de COV par un matériau argileux tunisien organo-modifié. *Journal de la Société Chimique de Tunisie*, **12**, 139-149.

[28] Sebei, H. (2013) Etude des interactions de polluants minéraux et organiques avec des matrices phosphocalciques. Thèse de doctorat de l'Université de Toulouse, Spécialité: Génie des procédés et de l'environnement, Toulouse.